Sea ice outlook 2010

Lars Kaleschke[1], Gunnar Spreen[2]
[1]Institute for Oceanography, KlimaCampus, University of Hamburg
[2]Jet Propulsion Laboratory, California Institute of Technology
Contact: `lars.kaleschke@zmaw.de`, Tel. ++49 40 42838 6518

July 14, 2010

1 Extent Projection

We estimate a September 2010 monthly mean extent of **5.2 ± 0.1 million square kilometers**.

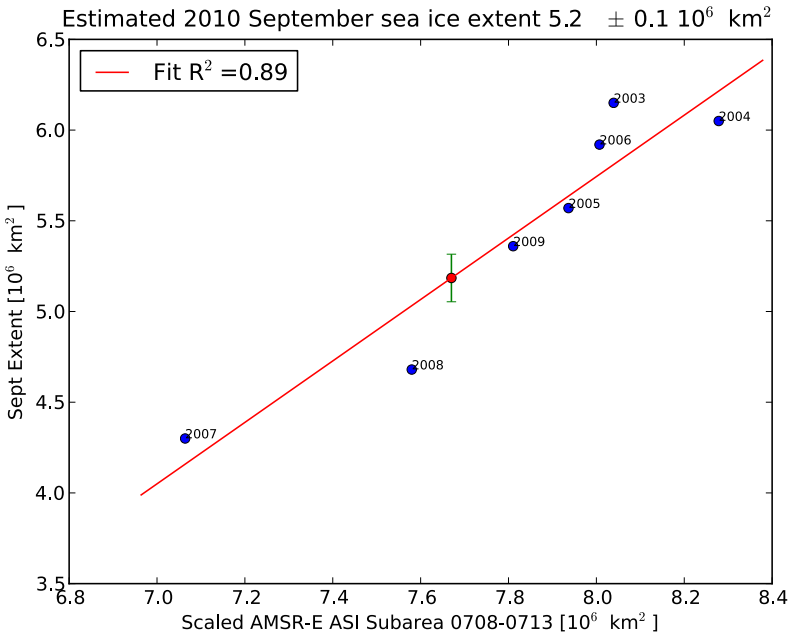

Figure 1: September 2010 sea ice extent estimate. Daily updates are available at `ftp://ftp-projects.zmaw.de/seaice/prediction/`

2 Methods and Techniques

The estimate is based on AMSR-E sea ice concentration data on a 6.25 km grid derived using the ARTIST sea ice (ASI) algorithm (Spreen et al., 2008; Kaleschke et al., 2001). We used two different sea ice concentration data sets, one based on the reprocessed gridded level 3 AMSR-E brightness temperatures for the years 2003-2010 (`ftp://ftp-projects.zmaw.de/seaice/AMSR-E_ASI_IceConc/`), the other is based on near-real-time AMSR-E level 1b brightness temperatures. Because the level 3 data is available only with some delay the level 1 data are used for the most recent year.

A five day median filter is applied on the data to reduce the atmospheric influence and coastal spillover effects (Kern et al., 2010; Maaß et al., 2010). Thus, any dates given below are not exactly for the individual day but include the previous four days.

To obtain an estimate we regress the ice area from the Arctic subregion shown in Figure 2 with the previous years and their September mean extents. As shown in Figure 2 the considered region contains the central Arctic and some of the Arctic marginal seas but excludes the multiyear sea ice region north of Greenland and the North Pole. To be able to regress the original AMSR-E sea ice area with the mean September sea ice extent two scalings are applied. First the 11-15 September five day median filtered sea ice area of the Arctic subregion for years 2003 to 2009 are regressed with the according mean September sea ice extent taken from NSIDC (Fetterer et al., 2002, updated 2009) (Figure 3). And second the near real time and reprocessed AMSR-E ice concentrations are scaled to each other to account for the small differences between the two datasets (Figure 4). Using these scalings the mean September sea ice extent is estimated from the current five day median sea ice area and the sea ice area of the same five day period of years 2003 to 2009 (Figure 1).

3 Rationale

Our assumption is that the Arctic sea ice is on decline with a constant trend over the last few years. In addition there is interannual variability due to the weather.

A hindcast experiment for last year was conducted to test the performance of the new method. The correlation between September mean extent and the selected training area increases as the time difference decreases. In 2009 the correlation R^2 increased from insignificant values earlier in Spring to values around $R^2 \approx 0.5$ at the the end of May (Figure 5).

The standard error of the prediction σ dropped from ± 4 million square kilometers to values below ± 1 million square kilometers after June 10 (Figure 6). As the deviation from the observed value is signifcantly smaller than the standard error we define its half as our uncertainty.

The prediction skill depends on the selected training area. The skill increased when we removed some of the seasonal ice covered areas in our analysis (Figure 6).

From this hindcast experiment we deduce that reliable forecasts seem to be possible in mid-June. Some predictive skill exists already at the end of May.

With the additional processing steps we considerably reduce the observational noise and improve the prediction skill as compared to our last years attempts using SSM/I data. The higher spatial resolution of AMSR-E compared to SSM/I allows to better resolve small scale sea ice openings like coastal polynyas. The size and number of these openings might inhere some predictive capability for the sea ice minimum. Which could explain parts of the improvement achieved in comparison to using SSM/I data.

4 Executive Summary

Our outlook is based on statistical analysis of satellite derived sea ice area. We introduced following improvements: high resolution (AMSR-E) sea ice concentration data, a time-domain filter that reduces observational noise, and a space-domain selection that neglects the outer seasonal ice zones. Thus, small scale sea ice openings like coastal polynyas that might inhere some predictive capability for the sea ice minimum can be better utilized.

References

Fetterer, F., K. Knowles, W. Meier, and M. Savoie (2002, updated 2009). *Sea Ice Index*, 1972-2009. Boulder, Colorado USA: National Snow and Ice Data Center. Digital media.

Kaleschke, L., C. Lüpkes, T. Vihma, J. Haarpaintner, A. Bochert, J. Hartmann, and G. Heygster (2001). SSM/I Sea Ice Remote Sensing for Mesoscale Ocean-Atmosphere Interaction Analysis, *Can. J. Rem. Sens.*, 27(5), 526-537.

Spreen, G., L. Kaleschke, and G. Heygster (2008). Sea ice remote sensing using AMSR-E 89-GHz channels, *J. Geophys. Res.*, 113, C02S03, doi:10.1029/2005JC003384.

Kern, S., L. Kaleschke, and G. Spreen (2010). Climatology of the Nordic (Irminger, Greenland, Barents, Kara and White/Pechora) Seas ice cover based on 85 GHz satellite microwave radiometry: 1992-2008.Tellus A, Published Online: Apr 19 2010, DOI: 10.1111/j.1600-0870.2010.00457.x

Maaß N., and L. Kaleschke (2010). Improving passive microwave sea ice concentration algorithms for coastal areas: applications to the Baltic Sea. Tellus A, Published Online: Apr 1 2010, DOI: 10.1111/j.1600-0870.2010.00452.x

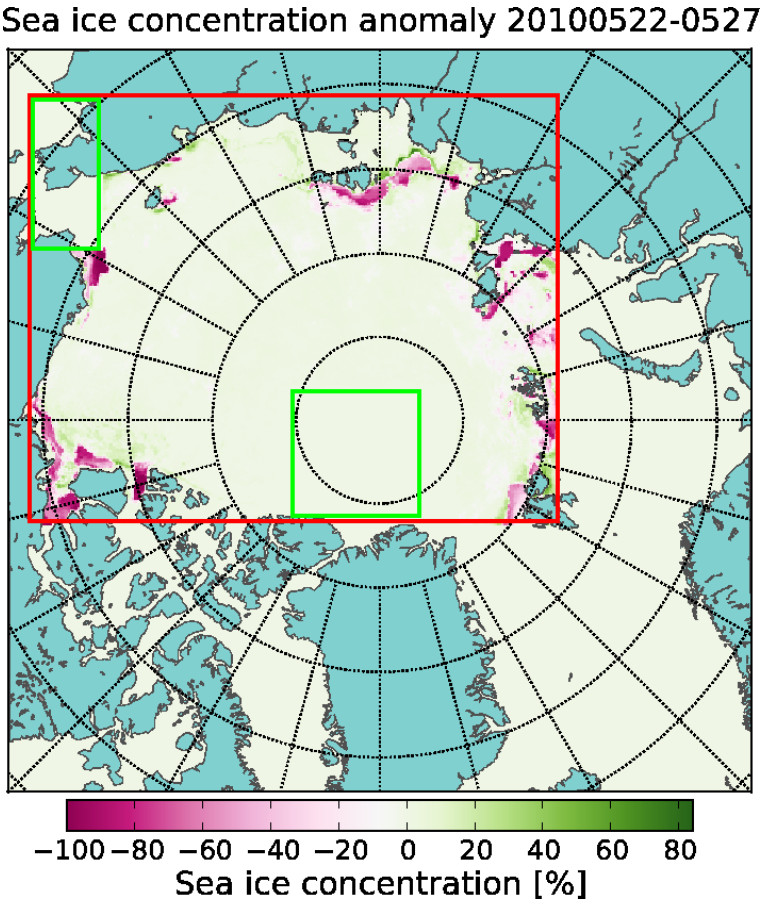

Figure 2: 2010 sea ice concentration anomaly derived from AMSR-E ASI data. The anomaly is calculated with respect to the years 2003–2009. The red rectangle indicates the subset for calculation of the ASI AMSR-E sea ice area. The green rectangles indicates areas that are not taken into account.

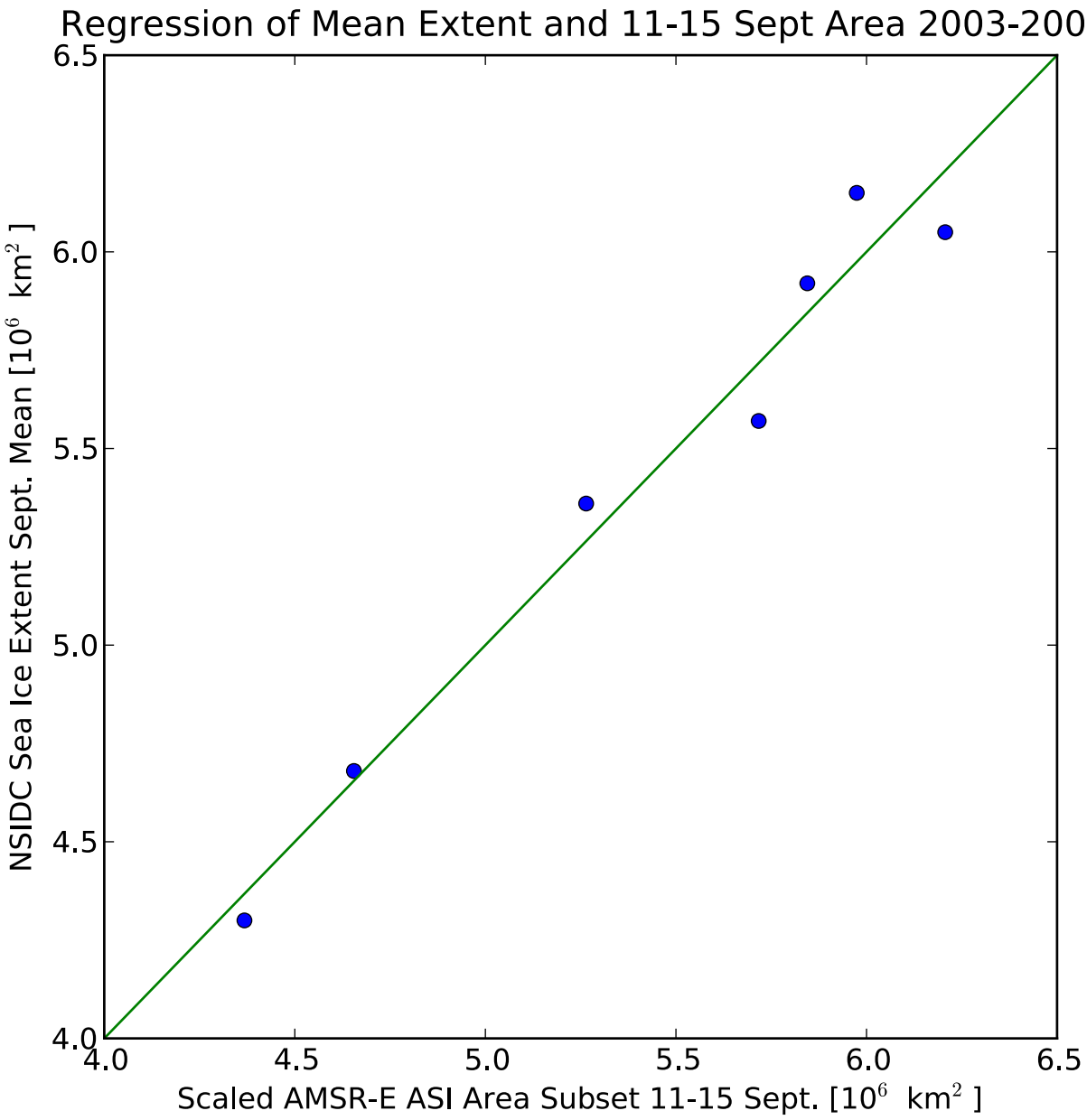

Figure 3: Regression of regional (region shown in Fig. 2) five-day median filtered AMSR-E ASI area and total NSIDC September mean extent.

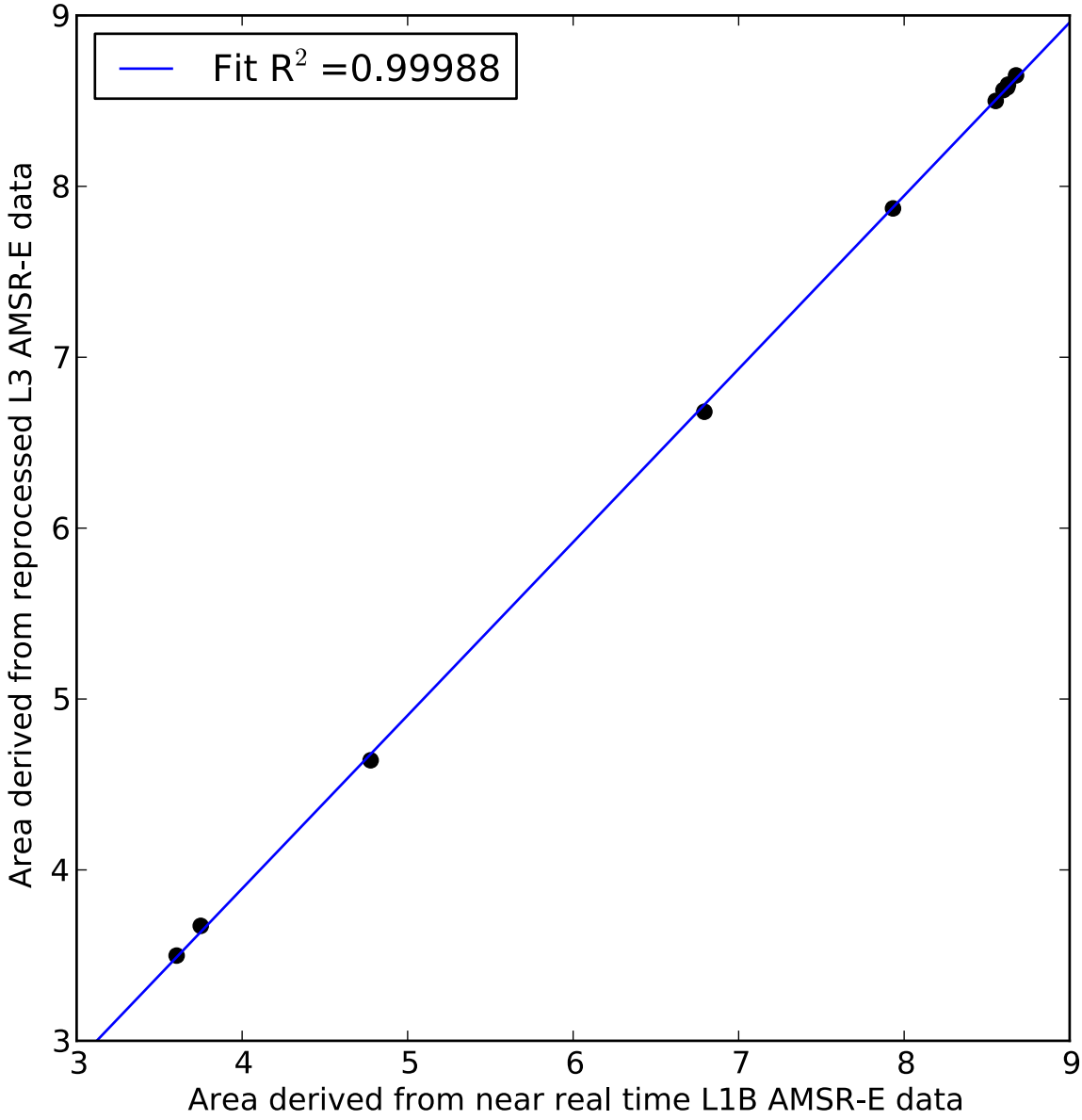

Figure 4: Regression of near real time and reprocessed data.

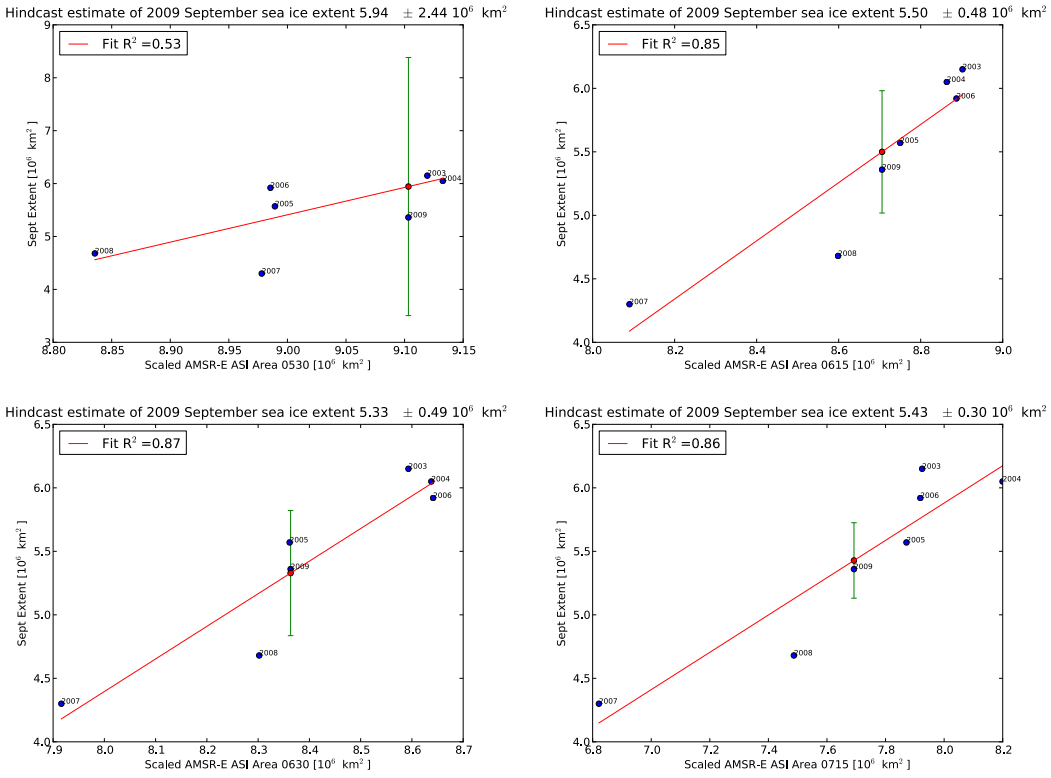

Figure 5: Hindcast prediction for September 2009.

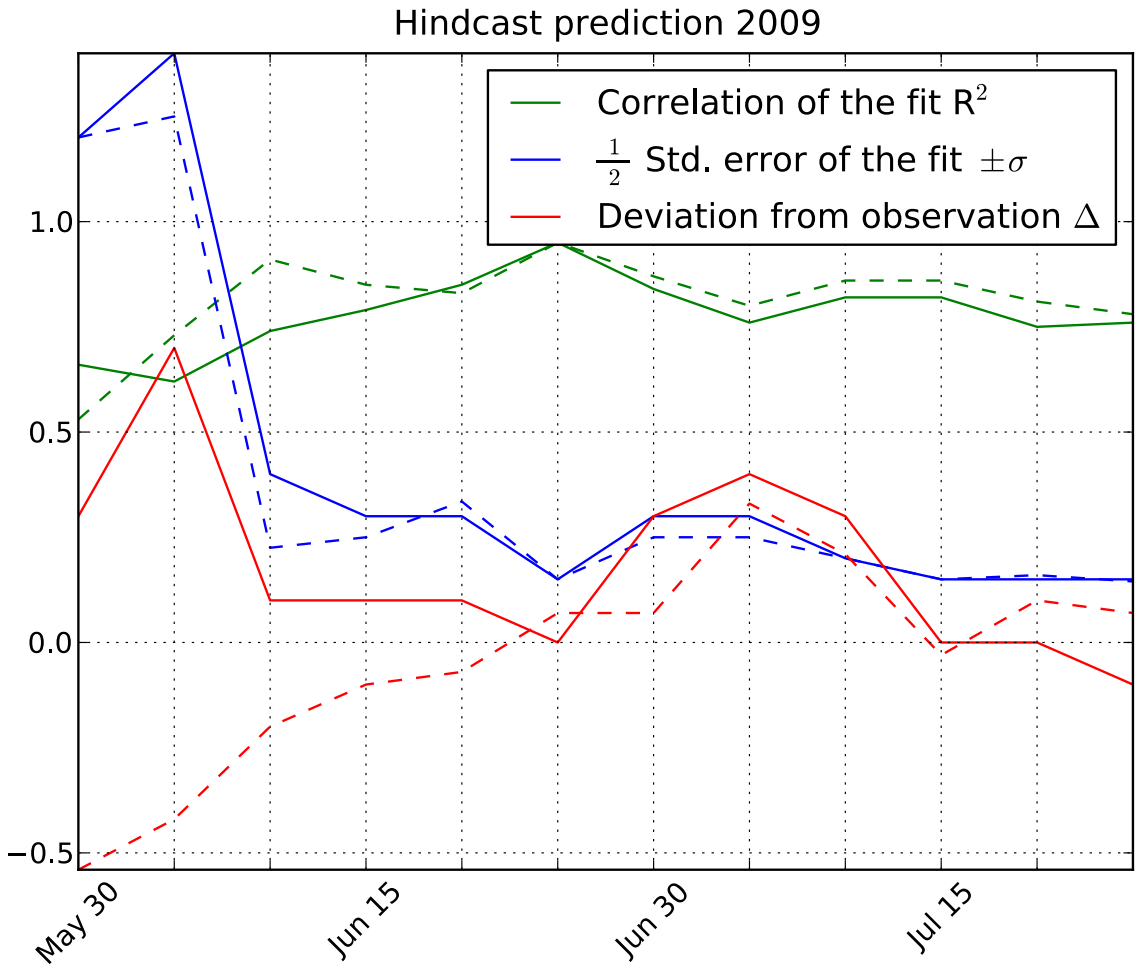

Figure 6: Hindcast prediction for September 2009. The results for the solid and dashed lines are for different training areas (see 2).

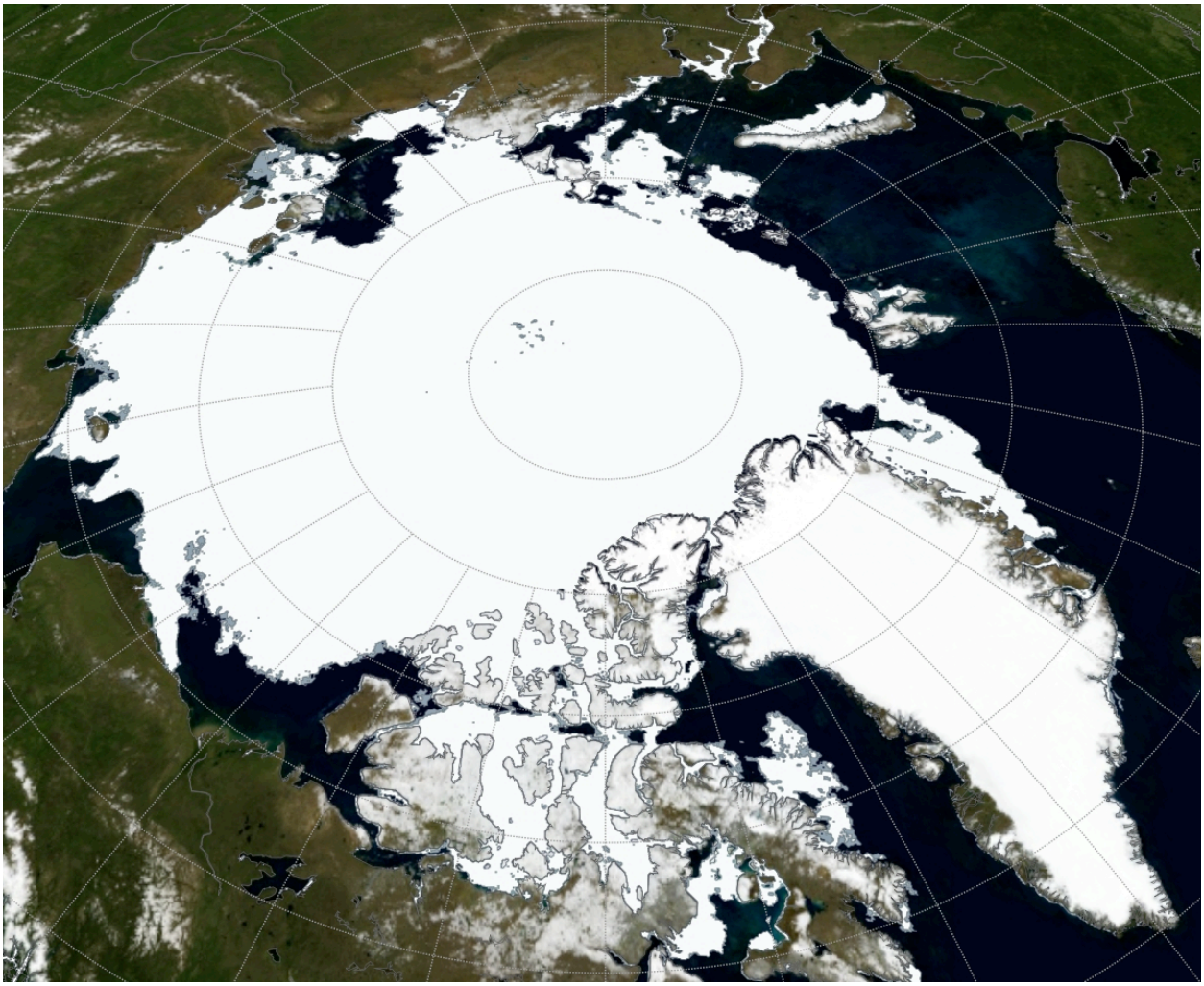

Recent AMSR-E map.